Long-Range Particles of $Z=1$ to 4 Emitted During the Spontaneous Fission of ^{252}Cf†

S. W. COSPER, J. CERNY, AND R. C. GATTI
Department of Chemistry and Lawrence Radiation Laboratory, University of California, Berkeley, California

(Received 6 October 1966)

The long-range particles emitted during the spontaneous fission of ^{252}Cf have been investigated, confirming the emission of ^{1}H, ^{2}H, ^{3}H, ^{3}He, ^{4}He, and ^{6}He. In addition it was found that ^{8}He, ^{6}Li, ^{7}Li, ^{8}Li, ^{9}Li, ^{9}Be, ^{10}Be, and probably other isotopes of Be are also emitted. A detailed search for the emission of the heavy-helium isotopes ^{7}He, ^{9}He, and ^{10}He yielded no evidence for their particle stability. Relative intensities and most probable energies for all emitted hydrogen and helium isotopes (except ^{3}He) and for the Li and Be ions were obtained.

1. INTRODUCTION

SEVERAL investigators have reported the observation of long-range protons,[1,2] deuterons,[1] tritons,[1–3,8] ^{3}He particles,[1] and α particles[1–7] emitted during the spontaneous fission of ^{252}Cf. In addition, Whetstone and Thomas[2] have reported the definite observation of ^{6}He particles (and possibly ^{8}He particles) from ^{252}Cf fission. These latter data suggest that particles with charge ≥ 2 and mass number >6 might also be produced during the fission process, although their production rate appears small compared with that of α particles.

Since all the known hydrogen isotopes which are stable to nucleon emission are emitted during the fission process, it seems reasonable to assume that all nucleon-stable helium isotopes could be observed during the fission of ^{252}Cf. The observation of ^{3}He, ^{4}He, and ^{6}He along with the absence of ^{5}He which is known to be particle unstable ($^{5}\mathrm{He} \rightarrow {}^{4}\mathrm{He}+n+0.957$ MeV)[9] tends to support this assumption. Thus, a detailed study of the long-range helium isotopes emitted during the spontaneous fission of ^{252}Cf might be expected to yield information concerning the particle stability of ^{7}He, ^{8}He, and ^{10}He. At present ^{7}He has been predicted to be nucleon unstable from a calculation based on a Coulomb correction to the known[10] $T=\frac{3}{2}$ states in ^{7}Li and ^{7}Be, while ^{8}He has been recently observed as a delayed-neutron emitter[11] and its mass has been measured.[12] In an effort to determine whether helium isotopes of mass number >8 exist, we have searched the long-range fragments from ^{252}Cf fission for the presence of ^{10}He, which due to neutron-pairing-energy systematics might be a better candidate for stability than ^{9}He.

Additionally, a knowledge of the various light fragments emitted during the spontaneous fission of ^{252}Cf, along with their relative intensities and energy distributions, might be of help in better understanding the mechanism of the fission process itself.

2. EXPERIMENTAL

The two sources used for these measurements consisted of 20 and 12 μg of ^{252}Cf, respectively, deposited on platinum backings and having a nominal source diameter of 0.3 cm. The 20-μg source was covered with a 6.66-mg/cm^2 aluminum foil and the 12-μg source with a 15.83-mg/cm^2 gold foil. Additional foils were added externally so that the total foil thicknesses were 8.26-mg/cm^2 of aluminum and 24.75 mg/cm^2 of gold, respectively, each sufficient to stop the 6.11-MeV α particles produced in the natural decay of ^{252}Cf. The positions of the source and external foil with respect to the detector assembly are shown in Fig. 1. The solid angle subtended by the detectors was 0.007 sr as

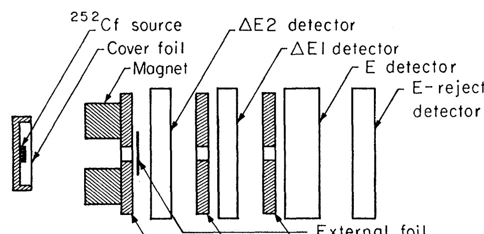

FIG. 1. Experimental arrangement of the ^{252}Cf source with respect to the cover foil, magnet, external foil, collimators and detectors.

† Work performed under the auspices of the U. S. Atomic Energy Commission.

[1] H. E. Wegner, Bull. Am. Phys. Soc. 6, 307 (1961).
[2] S. L. Whetstone, Jr. and T. D. Thomas, Phys. Rev. Letters 15, 298 (1965).
[3] J. C. Watson, Phys. Rev. 121, 230 (1961).
[4] R. A. Nobles, Phys. Rev. 126, 1508 (1962).
[5] M. L. Muga, H. R. Bowman, and S. G. Thompson, Phys. Rev. 121, 270 (1961).
[6] Z. Fraenkel and S. G. Thompson, Phys. Rev. Letters 13, 438 (1964).
[7] J. A. Coleman, A. W. Fairhall, and I. Halpern, Phys. Rev. 133, B724 (1964).
[8] D. L. Horrocks, Phys. Rev. 134, B1219 (1964).
[9] T. Lauritsen and F. Ajzenberg-Selove, Nucl. Phys. 78, 1 (1966).
[10] C. Détraz, J. Cerny, and R. H. Pehl, Phys. Rev. Letters 14, 708 (1965).
[11] A. M. Poskanzer, R. A. Esterlund, and R. McPherson, Phys. Rev. Letters 15, 1030 (1965).
[12] J. Cerny, S. W. Cosper, G. W. Butler, R. H. Pehl, F. S. Goulding, D. A. Landis, and C. Détraz, Phys. Rev. Letters 16, 469 (1966).

defined by the series of tantalum collimators. For certain runs the external foil was removed and the solid angle subtended by the counter telescope decreased to 0.0006 sr; this permitted the 6.11-MeV-decay α particles to strike the first detector, markedly increasing its counting rate.

After penetrating the cover foil, long-range particles from the source passed between the poles of a small magnet, which deflected most of the low-energy electrons, and traversed a detector telescope consisting of 3 (or 4) phosphorous-diffused and/or lithium-drifted silicon detectors, depending on the particles being studied and the method of data collection. The entire detector assembly was kept in a vacuum while data were being collected; however, $\sim$33 μg/cm^2 of air at 1-atm pressure was trapped between the cover foil and the ^{252}Cf source. All measured energies were corrected for losses in this air layer, the cover and external foils and the detector dead layers.

Following preamplification, pulses from the detectors were routed to delay-line shaped linear amplifiers with crossover pickoff. An abbreviated block diagram of the electronic equipment is shown in Fig. 2. A particle which traversed the two "ΔE" detectors and stopped in the "E" detector (i.e., particle 1 in Fig. 2) generated three pulses which were amplified and fed to a fast-slow coincidence system with a fast coincidence resolving time of 50 nsec. The pileup rejector section of the coincidence system was not employed unless specifically indicated in the text. If the coincidence requirements were met, these three pulses were presented to the particle identifier (PI) along with a timing pulse. Particles which did not stop in the "E" detector (i.e., particle 2 in Fig. 2) generated a pulse in the "E-reject"

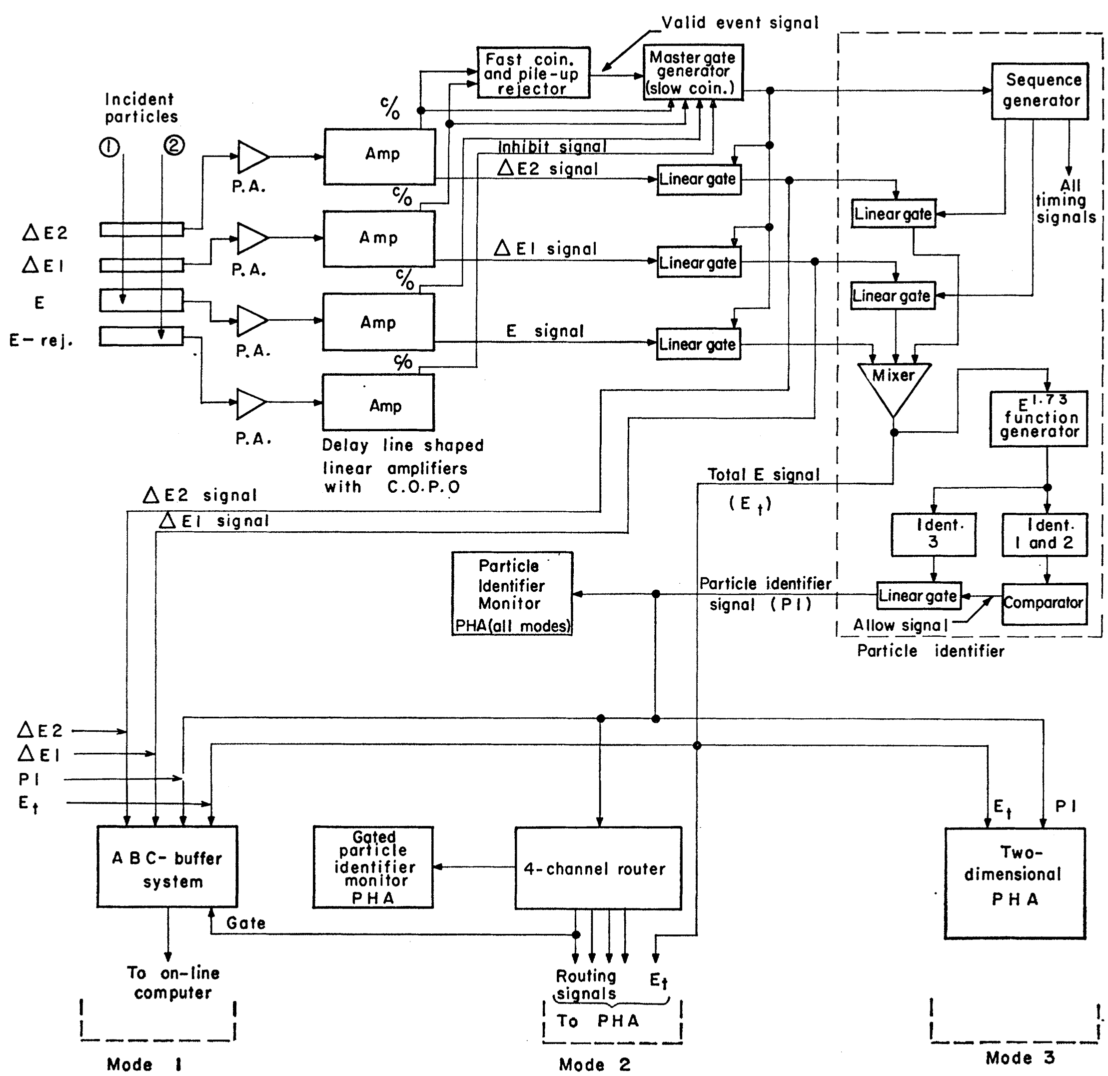

FIG. 2. An abbreviated block diagram of the electronic equipment.

detector which was used to reject the event in an anticoincidence circuit. This was necessary because particles which do not lose their entire energy in the first three detectors yield an improper identification pulse.

The particle identifier (PI) shown schematically in Fig. 2 was developed at this laboratory[13] and is an augmented version of an earlier model[14] also developed here. This new identifier, like its predecessor, generates an identification pulse based on an empirical relationship between the range of a particle, R, and its energy, E: $R=aE^{1.73}$. The proportionality constant a is different for the various particles, decreasing with increasing mass and charge. The three-counter identifier produces three identification pulses for each particle. A schematic derivation of these three pulses using the three energy pulses ($\Delta E2$, $\Delta E1$, and E) and the relationship $R=aE^{1.73}$ is presented in Fig. 3. It is seen that the identification signals are proportional to the $\Delta E2$, $\Delta E1$, and ($\Delta E2+\Delta E1$) detector thicknesses, respectively. The Ident. 1 and Ident. 2 pulses (see Figs. 2 and 3) are then compared. If their ratio agrees within preset adjustable limits, a linear gate is opened allowing the third identification pulse (Ident. 3 on Figs. 2 and 3) to emerge as the PI output. In the above manner events which produce an abnormal energy loss (due to blocking, channeling, etc.) in a single ΔE detector and which would therefore identify improperly are eliminated. Tests have shown that these "bad" events—which predominantly fill the valleys of the identifier spectrum—can be removed while 95 to 99% of the total counts are allowed through the particle identifier.

Typical PI spectra for hydrogen and helium isotopes obtained using the three-counter identifier described above are shown in Fig. 4. In these cases, ~2% of the total hydrogen isotope counts and ~3% of the total helium isotope counts were rejected. The three-counter identifier was designed so that it is also capable of being operated as a conventional two-counter identifier. The lower energy data presented in this report were taken with the PI operating in this mode (one ΔE detector, an E detector, and an E-reject detector).

Three methods of taking data were used in the course of this experiment (see Fig. 2):

Mode 1: To investigate relatively low-yield particles in detail, the $\Delta E2$, $\Delta E1$, ($\Delta E2+\Delta E1+E\equiv E_{\text{total}}$), and PI pulses were fed into a 4096-channel ADC (analog-

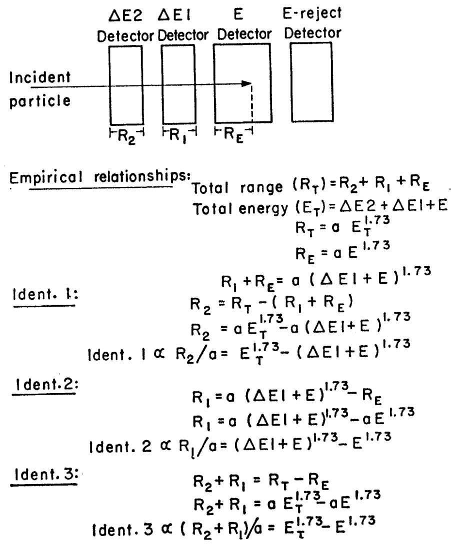

FIG. 3. A schematic derivation of the three identification pulses generated by the three-counter particle identifier.

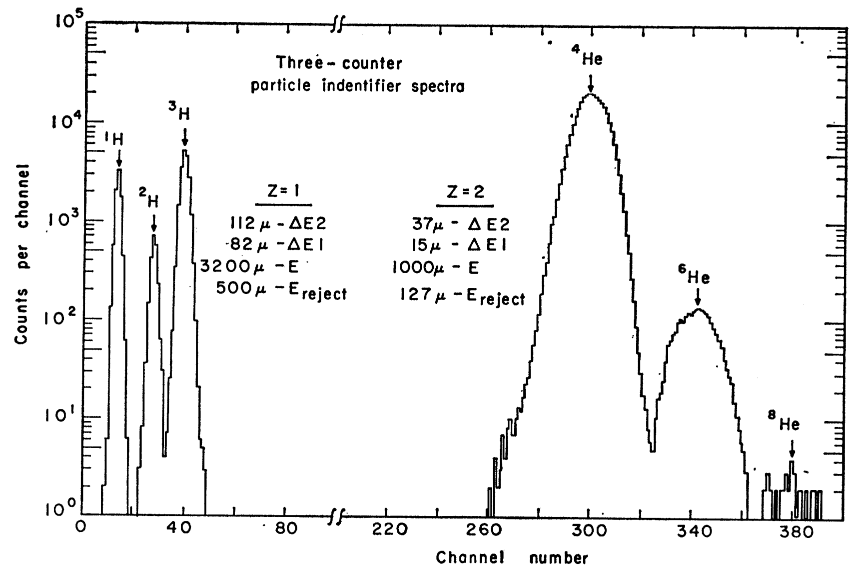

FIG. 4. Typical spectra from the three-counter particle identifier resulting from long-range particles emitted during ^{252}Cf fission. The thicknesses of the detectors which were used to accumulate these data are indicated.

[13] F. S. Goulding, D. A. Landis, J. Cerny, and R. H. Pehl, IEEE Trans. Nucl. Sci. NS-13, 514 (1966).
[14] F. S. Goulding, D. A. Landis, J. Cerny, and R. H. Pehl, Nucl. Instr. Methods 31, 1 (1964).

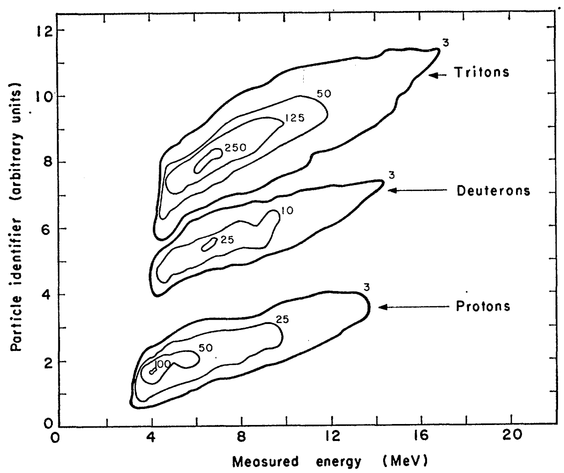

FIG. 5. A two-dimensional contour plot of a particle identifier versus total energy spectrum of the hydrogen isotopes emitted from ^{252}Cf fission.

to-digital converter)-Buffer system which was gated by the appropriate region of the PI spectrum. These four pulse heights were recorded in an on-line computer and were later individually analyzed using the known detector thicknesses and range-energy relations in silicon for the particles of interest. The range-energy relations which were used for the analysis of these individual events were coded at this laboratory[15] and agreed very well with available experimental data and prior computations.[16]

Mode 2: To collect the energy spectra of the more populous particles in their higher energy ranges, the particle identifier output was fed to a four-channel router. Four single-channel analyzers in the router were set around the peaks of interest in the PI spectrum and their outputs were used to route the energy signals into the appropriate quadrants of a 4096-channel pulse-height analyzer. In this manner the energy spectra of four particles could be collected simultaneously. To effect good separation of peaks in the PI spectrum, the energy loss in the E detector was normally required to be ≥ 3 MeV for hydrogen isotopes and ≥ 6 MeV for helium, lithium, and beryllium isotopes.

Mode 3: To investigate energy spectra at low energies, the particle identifier pulse and the total energy pulse were fed to a 4096-channel pulse-height analyzer operating in a two-dimensional (64×64 channels) mode. When taking two-dimensional data, no requirements were placed on the E signal, allowing the minimum energy possible to be recorded. A representative two-dimensional spectrum for the hydrogen isotopes is shown in Fig. 5.

The detectors used in this experiment were energy-calibrated by comparing a precision pulser with the energy losses of α particles from a ^{212}Po-^{212}Bi natural α source. The uniformities and thicknesses of the thin detectors were determined by observing the energy loss profiles of natural α particles and selected narrow energy bands of long-range α particles and ^{6}He particles from ^{252}Cf fission.

Since runs varying in duration from 7 to 220 h were required to collect the data presented in the following section, the energy calibration of the electronic equipment was frequently checked using a previously calibrated precision pulser. The entire system was very stable—typical drifts amounted to less than 0.5% over an entire run. While searching for rare events (operating in Mode 1), the entire system was energy calibrated every 3–4 h, thus insuring a reliable energy scale for those events.

In Table I are shown the various detector thicknesses and modes of collecting data which were used for the accumulation of the energy spectra of the various long-range particles emitted from ^{252}Cf. In addition, the energy range over which counts *could* have been observed and the ^{252}Cf source used are given for each case. The energy distributions presented in the following section were obtained by appropriately normalizing and combining data from the different runs.

In order to investigate the background counts produced by the intense neutron and gamma-ray flux from the ^{252}Cf source, a 25-h run using the three-counter particle identifier was made after a 0.63-cm Ta absorber was placed in the position normally occupied by the external foil (see Fig. 1). No particles other than low-energy protons were observed. The intensity and energy distribution of these protons are discussed in Sec. 3C.

3. RESULTS AND DISCUSSION

Although the primary purpose of this investigation was to search for the possible emission of helium isotopes of mass seven, eight, and ten from the spontaneous fission of ^{252}Cf, data on other long-range particles were also obtained. These data are presented in the following sections with a minimum of discussion though the information should be of some help in better understanding the fission process. Although long-range particles emitted during fission are thought to originate in the stretched "neck" region of the fissioning nucleus at the time of scission, this has been proven only for α particles.[17]

A. Tritons

Due to the complexity of the observed proton energy distribution (see Sec. 3C), the energy spectra of the hydrogen isotopes will be presented beginning with tritons in order to show the type of energy distribution

[15] C. Maples, Jr. and J. Cerny, Lawrence Radiation Laboratory Report No. UCRL-17214, 1967 (unpublished).

[16] C. Williamson and J. P. Boujot, *Tables of Range and Rate of Energy Loss of Charged Particles of Energy 0.5 to 150 MeV*, (Centre D'Etudes Nucleaires de Saclay, 1962); and L. C. Northcliffe, *Studies in Penetration of Charged Particles in Matter* (National Academy of Sciences—National Research Council, Washington, D. C., 1964), pp. 173–186.

TABLE I. List of detector thicknesses, modes of data collection (see text), observable energy ranges and ^{252}Cf source used in the various experimental configurations.

Detected particle	Observable energy range (MeV)	Mode of operation	Silicon detector thicknesses (μ) $\Delta E2$	$\Delta E1$	E	E-reject	Source (μg of ^{252}Cf)
Proton	2.0– 4.4[a]	2	15[b]		125	587	12
Proton	3.0– 8.6	2	37[b]		460	148	12
Proton	6.0–23.7	2	37	32	3045	148	12
Proton	4.0–23.7	3	37	32	3045	148	12
Deuteron	5.3–31.7	3	37	32	3045	148	12
Deuteron	8.7–33.0	2	112	82	3200	507	20
Triton	6.5–37.7	2	37	32	3045	148	12
Triton	9.2–39.3	2	112	82	3200	507	20
^{3}He	14.2–>50	1	82	37	1200	507	20
^{4}He	8.3–38.2	2	15[b]		612	127	20
^{4}He	14.4–>50	2	37	15	1000	127	20
^{6}He	10.0–13.8	3	15[b]		37	82	12
^{6}He	11.0–45.4	2	15[b]		612	127	20
^{6}He	15.7–>50	2	37	15	1000	127	20
^{8}He	9.3–11.0[a]	3	15[b]		37	148	12
^{8}He	12.0–15.1	3	15[b]		37	82	12
^{8}He	14.0–>50	2	34[b]		1000	127	20
^{8}He	17.3–24.8	1	37	15	112	127	20
^{8}He	17.3–>50	2	37	15	1000	127	20
Li ions	15.2–39.3[a,c]	2	15[b]		127	587	12
Li ions	20.0–>50[c]	2	15[b]		612	127	20
Li ions	24.0–41.9[c]	1	37	15	112	127	20
Be ions	23.0–>50[a,d]	2	15[b]		127	587	12
Be ions	28.8–>50[d]	2	15[b]		612	127	20
Be ions	38.0–>50[d]	1	37	15	112	127	20

[a] To effect these measurements, the external foil was removed and the solid angle subtended by the detectors was reduced from 0.007 to 0.0006 sr.
[b] Where only one value for the thickness of the ΔE detectors is listed, the equipment was being operated as a two-counter particle identifier system.
[c] The observable energy range given was calculated for ^{7}Li.
[d] The observable energy range given was calculated for ^{10}Be.

normally observed for long-range particles emitted during fission.

Tritons emitted from ^{252}Cf have been observed by Watson,[3] Wegner,[1] Horrocks,[8] and Whetstone and Thomas.[2] The triton energy spectrum resulting from this investigation is shown in Fig. 6(a); the distribution peaks at 8.0±0.3 MeV with a half-width at half-maximum (HWHM)[18] of 3.1±0.3 MeV. The maximum triton energy observed was 24.3 MeV, nearly 8 MeV higher than the previously reported maximum of 16.5 MeV.[3] Table II lists the results of this experiment along with those of other investigators who have observed tritons from ^{252}Cf. The triton intensities listed under the column labeled "extrapolated" result from extrapolating both the triton and α-particle energy spectra to zero energy as shown by the dashed lines on their respective energy distributions while the values listed under the column headed "measured" result from using only those portions of the energy spectra which were actually observed experimentally. This procedure is followed throughout. As can be seen from Table II, the present results for tritons are in accord with those of other investigators.

[17] E. K. Hyde, *The Nuclear Properties of the Heavy Elements III–Fission Phenomena* (Prentice-Hall, Inc., Englewood Cliffs, New Jersey, 1964).

[18] Half-width at half-maximum (HWHM) values are given for the energy distributions instead of full width at half-maximum (FWHM) values since the measured energy spectra usually do not extend to low enough energies for experimental FWHM values.

B. Deuterons

Although deuterons from ^{252}Cf have been observed by Wegner,[1] no energy distribution has been reported. This is in part due to their infrequent emission relative to most other long-range particles emanating from ^{252}Cf. The energy distribution of deuterons measured during this experiment is presented in Fig. 6(b). The error bars on the figure represent counting statistics only. The distribution peaks at 8.0±0.5 MeV, has a HWHM of 3.6±0.5 MeV and extends to 21.5 MeV. This information, along with relative intensity results, is listed in Table II where Wegner's values[1] are included for comparison.

C. Protons

Proton emission from ^{252}Cf has been reported by Wegner[1] and Whetstone and Thomas.[2] The proton energy distribution obtained from this investigation is presented in Fig. 7(a). It is unique among all the energy spectra measured in that it appears to be composed of three separate energy distributions. A possible decomposition of the proton energy spectrum into three components is shown in Fig. 7(b), where the curves are labeled A, B, and C. Utilizing the fact that both the deuteron and triton energy spectra exhibit a most probable energy of about 8.0 MeV with a HWHM of about 3.3 MeV, one might expect the proton distribution resulting from the same release mechanism to be similar. For this reason it appears that the proton

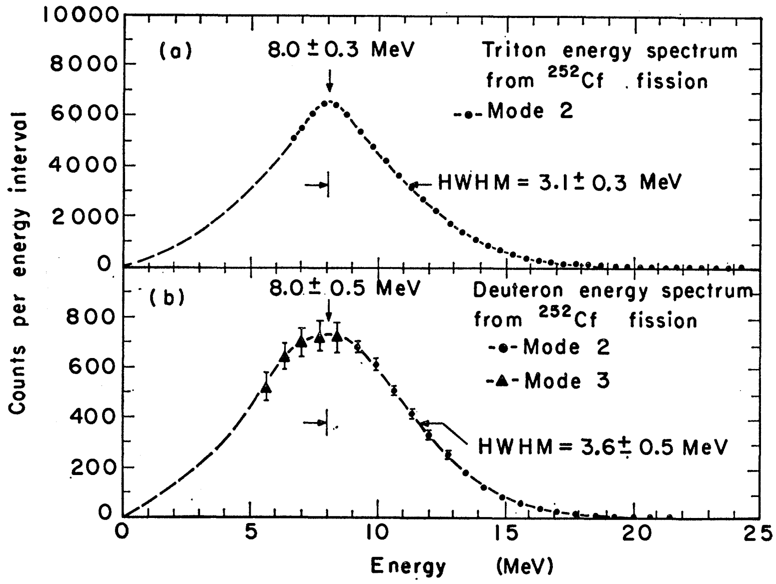

FIG. 6. Energy spectra of (a) tritons and (b) deuterons emitted from ^{252}Cf fission. The error bars represent counting statistics only; when no error bar is shown, the error is contained within the point.

component labeled A in Fig. 7(b) corresponds to protons emitted from ^{252}Cf during the fission process. This distribution peaks at 7.8±0.8 MeV, has a HWHM of 3.4±0.8 MeV and extends to 18.8 MeV—quite similar to the deuteron and triton energy spectra.

In order to determine whether the protons of components B and C in Fig. 7(b) were associated with the intense 6.11 MeV α-particle flux from the ^{252}Cf source, a 3×10^{10}-dpm (disintegrations/min) ^{242}Cm natural α-particle source (6.11 MeV) was chemically purified and packaged in a manner identical with the ^{252}Cf source. The ^{242}Cm source was covered with a 24.75-mg/cm^2 gold foil which was sufficient to stop the natural α particles. All long-range particles from this source (in a geometry identical to that used for the ^{252}Cf measurements) were then investigated. (The spontaneous fission rate of this ^{242}Cm source was calculated[17] to be $<10^{-5}$ of that for the ^{252}Cf sources.) Only protons were observed; their resulting energy distribution is shown in Fig. 8(a) and appears to arise from two superimposed energy distributions which are labeled B and C. The shape and most probable energy of the proton distribution *B* from the ^{242}Cm source is almost identical to that of component *B* in the observed proton spectrum from ^{252}Cf [see Fig. 7(b)], while that portion of the proton distribution labeled C in Fig. 8(a) corresponds reasonably well with the high-energy part of the ^{252}Cf proton distribution labeled *C* in Fig. 7(b) (also see following paragraph). The low-energy portion (<3 MeV) of component *C* in Fig. 8(a) could not be investigated because of the thickness of the gold cover foil. The above similarities strongly indicate that proton components B and C observed from the ^{252}Cf source [Fig. 7(b)] arise primarily from the (α,p) reaction on either contaminants in the source or the air layer beneath the cover foil.

To investigate the effect of the high neutron (and gamma) flux on the counter telescope and the Ta collimators, a 0.63-cm Ta absorber was placed between the ^{252}Cf source and the detectors. No particles other

TABLE II. Numerical data derived from the energy spectra of the hydrogen isotopes emitted during the fission of ^{252}Cf.

Detected particle	Measured energy range (MeV)	Intensity relative to emission of 100 α particles[a] Measured[b]	Extrapolated[c]	Most probable energy (MeV)	HWHM (MeV)	No. of particles observed
Tritons[d]	6.5–24.3	6.42±0.20	8.46±0.28	8.0±0.3	3.1±0.3	75 700
Tritons[e]	3.7–16.5	6.7 ±1.1	···	8.0	3.5	34
Tritons[f]	5.5–16.0	6.0 ±0.5	···	8.5±1.0	···	>100
Tritons[g]	···	6.7 ±0.2	···	···	···	···
Deuterons[d]	5.3–21.5	0.63±0.03	0.68±0.03	8.0±0.5	3.6±0.5	5600
Deuterons[f]	···	<0.5	···	···	···	···
Protons[d]	7.3–18.8	1.10±0.15	1.75±0.30	7.8±0.8	3.4±0.8	26 900
Protons[f]	5.5–16.0	2.2 ±0.5	···	8.5±1.0	···	···

[a] 299 fissions/α-particle is the best available value for ^{252}Cf. See Ref. 4.
[b] Numerical values under this column were obtained by using only those portions of the energy spectra which were determined experimentally.
[c] Numerical values under this column were obtained by using energy spectra extrapolated to zero energy as shown on the individual energy distribution graphs.
[d] Results of this investigation.
[e] Results of Watson, see Ref. 3.
[f] Results of Wegner, see Ref. 1.
[g] Results of Horrocks, see Ref. 8.

than low-energy protons were detected. The energy distribution of these protons, which are assumed to arise primarily from the (n,p) reaction on the Ta absorber and/or the first detector, is shown in Fig. 8(b). The collection times of the two proton distributions shown in Fig. 8 are identical. Although the emission intensity observed in this manner is almost negligible, normal experimental conditions would allow protons resulting from (n,p) reactions on source contaminants and the gold cover and external foils to contribute significantly to the observed proton distribution [Fig. 7(a)]. Protons of this origin could account for the slight differences observed between distributions B and C on Figs. 7(b) and 8(a).

D. ^{4}H and ^{5}H

No evidence for the emission of hydrogen isotopes of mass 4 or 5 from ^{252}Cf was observed in any of the many particle identifier spectra discussed herein. This result is taken as additional evidence[19] that these isotopes are not stable to nucleon emission.

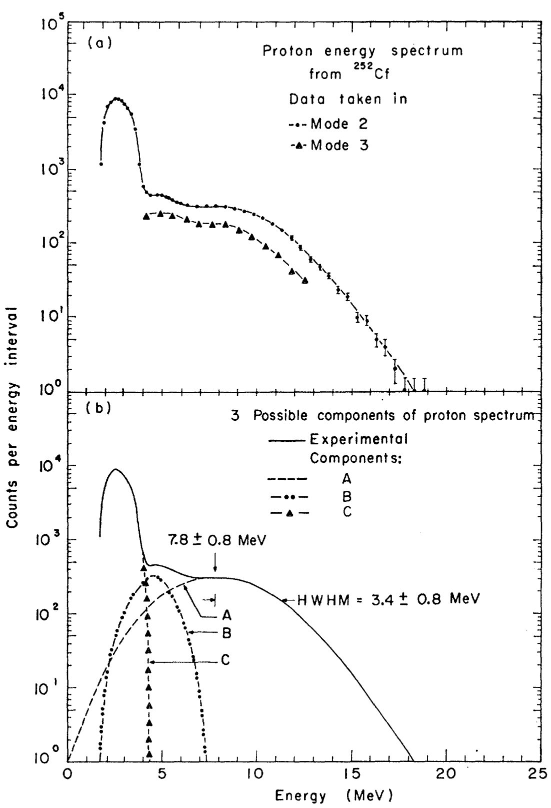

FIG. 7. Energy distribution of protons emitted from the ^{252}Cf source. Part (a) shows the experimental data and part (b) a possible decomposition of the spectrum into three components (see text for discussion).

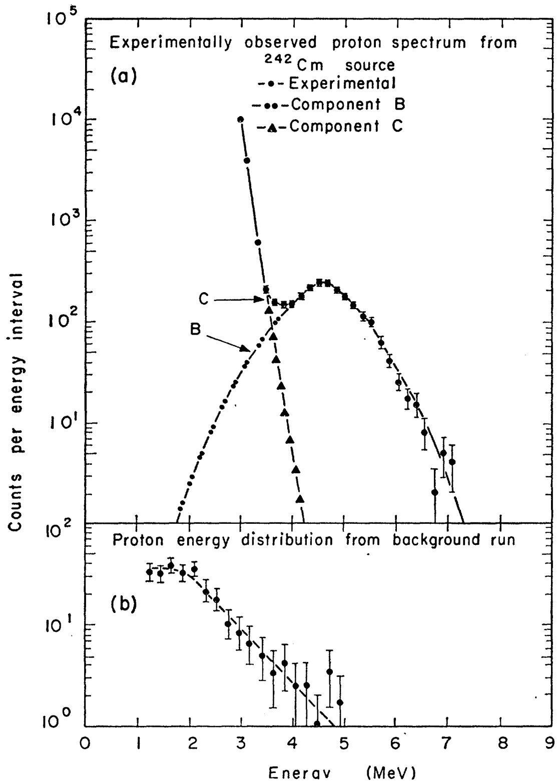

FIG. 8. The observed proton energy distributions from (a) the ^{242}Cm α source and (b) a background run in which a 0.63 cm Ta absorber was placed between the ^{252}Cf source and the detectors. Distribution (a) is decomposed into two possible components labeled B and C.

E. ^{3}He

The probable observation of ^{3}He particles emitted during the fission of ^{252}Cf with an intensity of <0.5 per 100 long-range α particles has been reported by Wegner.[1] All identifier spectra obtained in this investigation lacked a peak in the position expected for ^{3}He, although the slight tailing of the very intense α-particle peak could have obscured a very weak ^{3}He group. An expanded PI spectrum arising from the setup for the below experiment and showing the position of the predicted ^{3}He peak is presented in Fig. 9. In order to investigate in detail the extent to which ^{3}He was emitted from ^{252}Cf fission, energy pulses for particles whose identifier signal fell in the region between A and B on Fig. 9 were collected in Mode 1 and each event individually analyzed (see Sec. 3H). Of the 63 events which were recorded, 16 were definitely established as ^{3}He particles and 20 more as very probable ^{3}He particles. During the time interval required to accumulate these 63 events, 48,071 α particles were recorded, yielding an upper limit for the ^{3}He/α-particle ratio of 7.5×10^{-4}. The relevant ^{3}He numerical data are given in Table III.

F. α Particles

Many investigators have observed long-range α particles from ^{252}Cf fission.[1–7] Since approximately 88%

[19] A. I. Baz, V. I. Goldanskii, and Ya. B. Zeldovich, Usp. Fiz. Nauk **85**, 445 (1965); [English transl.: Soviet Phys.—Usp. **8**, 177 (1965)], and references therein.

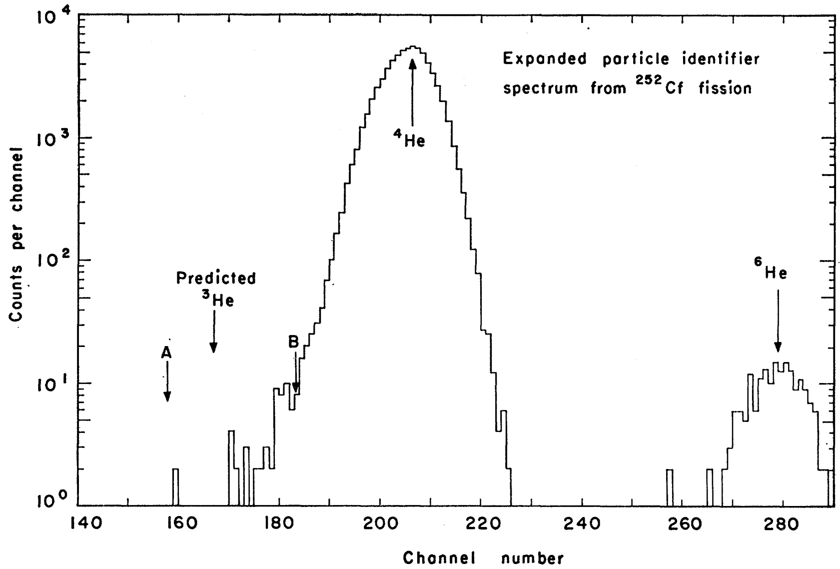

FIG. 9. An expanded particle-identifier spectrum showing the expected position of a ^{3}He peak. The region of the spectrum between A and B was investigated in detail (see Sec. 3E).

of all long-range particles emitted during the fission of ^{252}Cf are α particles, they have been studied in much greater detail than the other emitted particles. The energy distribution of α particles resulting from this investigation is shown in Fig. 10(a). This spectrum appears very symmetric about the peak energy of 16.0±0.2 MeV with a full width at half-maximum of 10.2±0.3 MeV. The highest energy α particle observed was 37.7 MeV, almost 4 MeV higher than had been previously reported.[5] Table III lists the data from the present experiment along with the results of some other investigations. The results of this experiment are in substantial agreement with most previous work.

G. ^{6}He

Whetstone and Thomas[2] have reported the emission of ^{6}He from ^{252}Cf fission. The ^{6}He energy distribution of the present investigation [shown in Fig. 10(b)] complements their results by extending the measurements from 13.5 MeV down to 10.0 MeV. This distribution is seen to peak at 12.0±0.5 MeV, has a HWHM of 4.0±0.5 MeV and extends to 33.3 MeV. Relevant numerical data for this isotope are tabulated in Table III.

H. ^{7}He and ^{8}He

The possible observation of ^{8}He particles emitted from ^{252}Cf has been reported by Whetstone and Thomas,[2] although their results could not be considered conclusive. While this experiment was in progress, the particle stability of ^{8}He was successfully demonstrated by Poskanzer *et al.*[11] and Cerny *et al.*[12] We have definitely established the emission of ^{8}He particles from ^{252}Cf

TABLE III. Numerical data derived from the energy spectra of the helium isotopes emitted during the fission of ^{252}Cf.

Detected particle	Measured energy range (MeV)	Intensity relative to emission of 100 α particles[a] Measured[b]	Extrapolated[c]	Most probable energy (MeV)	HWHM (MeV)	No. of particles observed
^{3}He[d]	14.2–21.3	$\leq$0.075	···	···	···	$\leq$36
^{3}He[e]	···	<0.5	···	···	···	···
^{4}He[d]	8.3–37.7	···	···	16.0±0.2	5.1±0.2	1 558 000
^{4}He[f]	11.4–34.0	···	···	~16.0	~5.5	~20 000
^{4}He[g]	6.5–31.0	···	···	~16.0	~7.5	445
^{4}He[h]	1.5–29.0	···	···	17.0±1.0	~5.5	~20 000
^{4}He[i]	8.0–34.0	···	···	~19.0	~5.0	~200
^{4}He[j]	10.0–~30.0	···	···	~15.0	~6.5	···
^{4}He[k]	10.0–30.0	···	···	~16.0	~5.0	~600
^{6}He[d]	10.0–33.3	1.95 ±0.15	2.63 ±0.18	12.0±0.5	4.0±0.5	71 300
^{6}He[f]	13.5–24.0	1.45 ±0.13	~2.0	···	···	119
^{8}He[d]	9.3–27.7	0.062±0.008	0.090±0.012	10.2±1.0	4.0±1.0	1110

[a] 299 fissions/α particle is the best available value for ^{252}Cf. See Ref. 4.
[b] Numerical values under this column were obtained by using only those portions of the energy spectra which were determined experimentally.
[c] Numerical values under this column were obtained by using energy spectra extrapolated to zero energy as shown on the individual energy distribution graphs.
[d] Results of this investigation.
[e] Results of Wegner, see Ref. 1.
[f] Results of Whetstone and Thomas, see Ref. 2.
[g] Results of Watson, see Ref. 3.
[h] Results of Nobles, see Ref. 4.
[i] Results of Muga *et al.*, see Ref. 5.
[j] Results of Fraenkel and Thompson, see Ref. 6.
[k] Results of Coleman *et al.*, see Ref. 7.

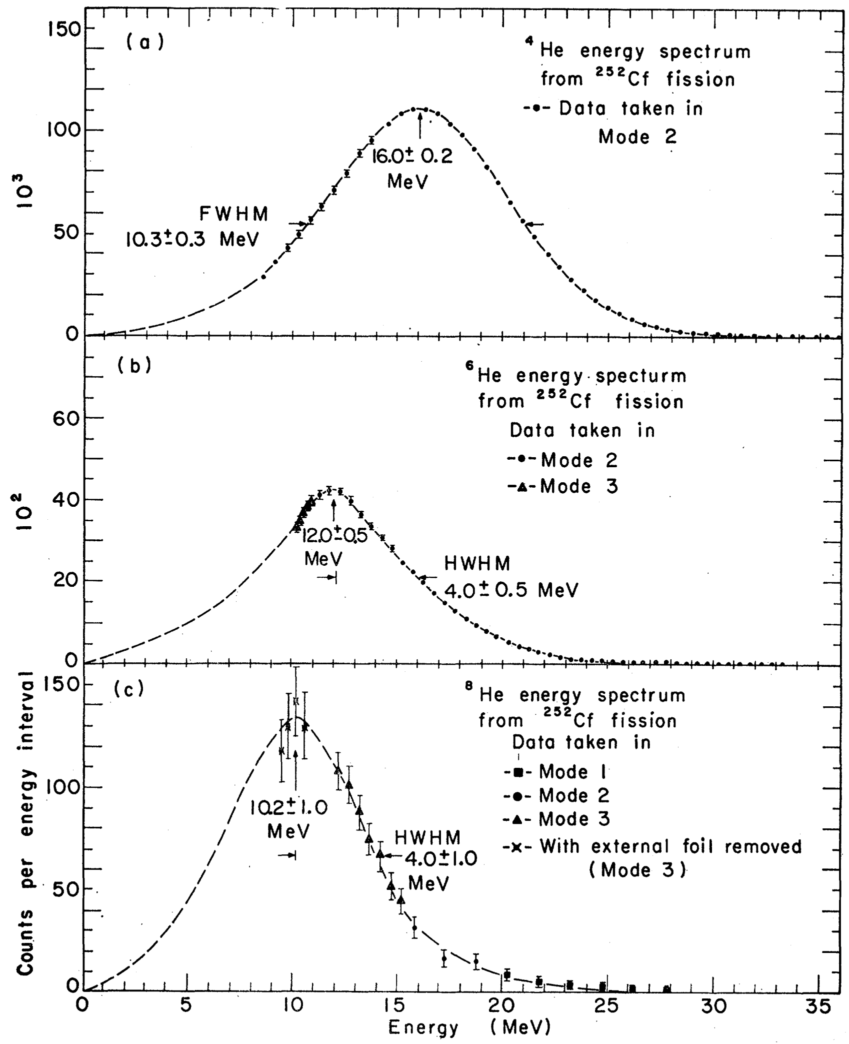

FIG. 10. Energy spectra of long-range (a) ^{4}He, (b) ^{6}He, and (c) ^{8}He particles emitted from ^{252}Cf fission. The error bars represent counting statistics only.

fission and have observed $\sim$1100 of these long-range events.

To investigate in detail the emission of helium isotopes with mass number ≥ 7, the three-counter identification system described in Sec. 2 was used to take data in Mode 1 using a counter telescope consisting of four fully-depleted phosphorous-diffused silicon transmission detectors (37 μ-$\Delta E2$; 15 μ-$\Delta E1$; 112 μ-E; and 127 μ-E-reject). Detector profiles were obtained for the somewhat nonuniform 37- and 15-μ detectors as described in Sec. 2. The $\Delta E2$, $\Delta E1$, E_{total}, and PI pulses were then individually recorded for 100 events whose identifier signal was contained in the ^{7}He$\rightarrow$^{9}He region of the identifier spectrum. The percentage deviation of each ΔE detector pulse from that expected for a ^{6}He, ^{7}He, ^{8}He, or ^{9}He particle of incident energy E_{total} was calculated for each event using range-energy relationships in silicon[15] and the *average* detector thickness. Taking into account the detector profiles, the probability of that event being a ^{6}He, ^{7}He, ^{8}He, or ^{9}He particle was calculated for each of the two ΔE detectors. The over-all probability that a particular event was either a ^{6}He, ^{7}He, ^{8}He, or ^{9}He was assumed to be the product of the respective probabilities for that particle in each detector; the event was finally classified according to its dominant probability.

Of these 100 events, 87 were definitely ^{8}He particles; the remaining 13 were randomly distributed among ^{6}He, ^{7}He, and ^{9}He and were attributed to background arising from:

(a) The relatively high intensity of the ^{6}He peak ($\sim$70 times more intense than the ^{8}He peak under these experimental conditions) permitting ^{6}He particles with abnormally high energy losses in *both* ΔE detectors to simulate ^{7}He.

(b) Chance coincidences between two α particles with appropriate relative energies and timing, which can simulate anything from ^{6}He to ^{6}Li. At the time these 100 events were accumulated, the pileup rejector shown in Fig. 2 was not in the circuit. Even though a

50-nsec fast coincidence was required between the crossover pickoff signals from the three detectors, it was found that two α particles of appropriate energies traversing the counter telescope within a time $\Delta t \leq 400$ nsec could satisfy the fast coincidence requirements because the crossover points of all three energy signals were shifted in the same direction by approximately the same amount. Tests indicated that, in the 46 h required to accumulate the 100 individual events, we could expect $\sim$4 to 9 counts in the ^{7}He through ^{9}He region due to this phenomenon.

(c) Chance coincidences of α-particles with protons, deuterons and tritons, which can simulate ^{7}He, ^{8}He, and ^{9}He, respectively.[12] Due to the much greater number of protons and tritons observed as compared to deuterons ($\sim$10 to 1 for both protons and tritons; see Secs. 3A, 3B, and 3C) this effect would yield $\sim$10 times more simulated ^{7}He and ^{9}He particles than ^{8}He particles. The chance rate in this experiment for such coincidences is small; in 46 h one would expect ≤ 1 α-p and ≤ 1 α-t chance coincidence of this type. Consequently, one would expect essentially no α-d chance coincidences which simulate ^{8}He particles.

These data were then supplemented by longer runs without individual energy analysis (i.e., Modes 2 and 3). The energy spectrum of ^{8}He particles emitted from ^{252}Cf fission is shown in Fig. 10(c), and the relevant numerical data are tabulated in Table III. The lowest energy portion of the ^{8}He distribution shown in Fig. 10(c) was obtained in Mode 3 with the external gold foil removed (see Fig. 1). These data did not overlap data taken with the external foil in place, and hence the normalization of these points [denoted with an X in Fig. 10(c)] to the higher energy data is less certain than for the other cases in which there was an overlap between the high- and low-energy data.

Under the experimental conditions of the above Mode 1 run, the relative intensity of emission of helium isotopes of $A \geq 4$ decreased by a factor of $\sim$110 for ^{6}He relative to ^{4}He and by a factor of $\sim$70 for ^{8}He relative to ^{6}He. From this trend one might expect the intensity of emitted ^{7}He to be $\sim$9 times that of ^{8}He. No ^{7}He emission of this intensity was observed experimentally and an upper limit for its emission can be set at $\frac{1}{12}$ the ^{8}He intensity.[20] We take this as strong evidence for the particle instability of ^{7}He which was predicted in Ref. 10.

A weak upper limit of 1 ^{9}He per 30 ^{8}He particles emitted from ^{252}Cf fission can be set from these data; however, the following section presents data which allow a more stringent limit to be placed on ^{9}He emission.

I. ^{10}He

As indicated in Sec. 1, if ^{10}He were particle-stable we would expect it to be emitted during ^{252}Cf fission. The three-counter identifier system was set up to record data in Mode 1 using the same detector telescope as was used for the detailed ^{7}He-^{8}He study (see Sec. 3H). Based on the systematics of the relative intensities and the most probable energies for the observed even-mass helium isotopes, we would expect under these conditions at least 1 ^{10}He for 70 ^{8}He particles, or about one ^{10}He event every 32 h. As described in the previous section, background events arising from α-α chance coincidences would completely mask a counting rate of this magnitude. The pileup rejector shown in Fig. 2 was designed to decrease this background. With the pileup rejector, events which consisted of two particles traversing the detector telescope with relative timing ≥ 75 nsec were rejected. Tests after installation showed that the background in the ^{10}He region of the particle identifier spectrum was reduced to approximately one count every 500 h, giving a possible true-to-chance ratio of $\sim$15 for ^{10}He events.

A continuous 220-h study of particles whose PI signal was contained in the $^9\text{He} \rightarrow {}^{10}\text{He}$ portion of the identifier spectrum yielded four events. Individual analysis (as described in the preceding section) showed that the most probable assignments for these events were three ^{9}He particles and one ^{10}He particle. The one ^{10}He event is within the expected background counting rate from α-α chance coincidences and well below the lower limit of seven expected counts for the 220-h period. The three probable ^{9}He events are also within the expected background counting rate from (a) α-α chance coincidences and (b) ^{8}He particles with abnormally high-energy losses in both ΔE detectors which could simulate a ^{9}He.

These data, along with the relative intensity and energy systematics of the helium isotopes emitted from ^{252}Cf fission, provide reasonable evidence for the particle instability of ^{10}He. Very recently, ^{10}He has been predicted to be unbound to $^8\text{He}+2n$ by $\sim$10 MeV.[21] In addition, the present results set an upper limit for the emission of ^{9}He at 1 ^{9}He/160 ^{8}He particles; since about 1 ^{9}He/9 ^{8}He particles would be expected from the systematics, these data also indicate the particle instability of ^{9}He.

J. Li and Be

The possible observation of Li and Be ions emitted from ^{252}Cf fission has been reported[2]; however, the authors state that the identification of these particles is not very certain. We have observed $\sim$2500 Li and $\sim$2250 Be ions emitted from the fission of ^{252}Cf. In addition, 100 individual Li-ion events of energy ≥ 24

[20] Even if the emission of paired neutrons in ^{252}Cf fission is preferred, one would certainly expect the intensity of emitted ^{7}He particles to be greater than or equal to that for ^{8}He particles.

[21] G. T. Garvey and I. Kelson, Phys. Rev. Letters **16**, 197 (1966).

TABLE IV. Numerical data derived from the energy distributions of the lithium and beryllium isotopes emitted during the fission of ^{252}Cf.

Detected particle	Measured energy range (MeV)	Intensity relative to emission of 100 α particles[a] Measured[b]	Extrapolated[c]	Most probable energy (MeV)	HWHM (MeV)	No. of particles observed
^{6}Li	24.0–33.2	0.0011±0.0005	...	...	...	10
^{7}Li	25.4–38.3	0.0081±0.0012	...	...	...	69
^{8}Li	26.8–37.5	0.0015±0.0006	...	...	...	13
^{9}Li	28.1–37.1	0.0009±0.0004	...	...	...	8
Li ions	15.2–37.3	0.126 ±0.015	0.132±0.016	20.0±1.0	3.3±1.0	2496
^{9}Be	39.3–43.9	~0.0002	...	...	...	2
^{10}Be	41.0–45.6	~0.0004	...	...	...	4
Be ions	23.0–49.1	0.156 ±0.016	0.201±0.020	~26.0	~5.5	2264

[a] 299 fissions/α particle is the best available value for ^{252}Cf. See Ref. 4.
[b] Numerical values under this column were obtained by using only those portions of the energy spectra which were determined experimentally.
[c] Numerical values under this column were obtained by using energy spectra extrapolated to zero energy as shown on the individual energy distribution graphs.

MeV [^{6}Li] were accumulated using the three-counter particle identifier and Mode 1 operation (see Sec. 2). An analysis of these events identical to that described in Sec. 3H showed that the composition of these 100 Li ions was as follows: 10-^{6}Li; 69-^{7}Li; 13-^{8}Li; and 8-^{9}Li particles. Thus, it appears that about 70% of these higher energy Li ions emitted during ^{252}Cf fission are ^{7}Li. During the 90 h required to accumulate the 100 Li events, 6 individual Be ion events of energy ≥ 38 MeV [^{9}Be] were also recorded. Analysis revealed that 2 were ^{9}Be and 4 were ^{10}Be particles. The reconstructed PI spectrum resulting from these individual events taken in Mode 1 is shown in Fig. 11(a). It can be seen that the lithium isotopes are well separated by the three-counter particle identifier.

The Mode 1 data on Li and Be ions were supplemented by longer runs using the two-counter particle identifier, Mode 2 data accumulation and a thin (15 μ) ΔE detector. A PI spectrum showing the separation of Li and Be ions obtained with the two-counter PI (external foil in place) is shown in Fig. 11(b). The expected positions for the various isotopes of Li and Be are indicated on the figure, but no separation of these isotopes was possible due to the nonuniformity of the ΔE detector.[22] Because of this, the energy spectra presented in Fig. 12 are for all Li isotopes (a) and for all Be isotopes (b); absorber corrections to the energy distributions were made for ^{7}Li and ^{10}Be, respectively. In addition, the energy spectrum resulting from the 69 individual ^{7}Li events previously discussed is shown as an inset in Fig. 12(a). In an attempt to determine the most probable energy for the Li and Be ions, the external gold foil was removed allowing the lower portion of the energy spectra to be extended. Relevant numerical data for the Li and Be isotopes emitted from ^{252}Cf fission are tabulated in Table IV.

[22] The behavior of this type of particle identifier in separating heavy ions is discussed by J. Cerny, S. W. Cosper, G. W. Butler, H. Brunnader, R. L. McGrath, and F. S. Goulding, Nucl. Instr. Methods **45**, 337 (1966).

K. Particles with $Z=5, 6$

The expected positions for boron and carbon groups are indicated on the PI spectrum presented in Fig. 11(b). Only boron ions ≥ 33 MeV [^{10}B] and carbon ions ≥ 43 MeV [^{12}C] could have been detected under the experimental conditions which prevailed when the data of Fig. 11(b) were taken. No significant intensity of these ions was observed; it should be noted that the two-counter PI (which has a much higher background counting rate than the three-counter PI) was used for accumulating these data.

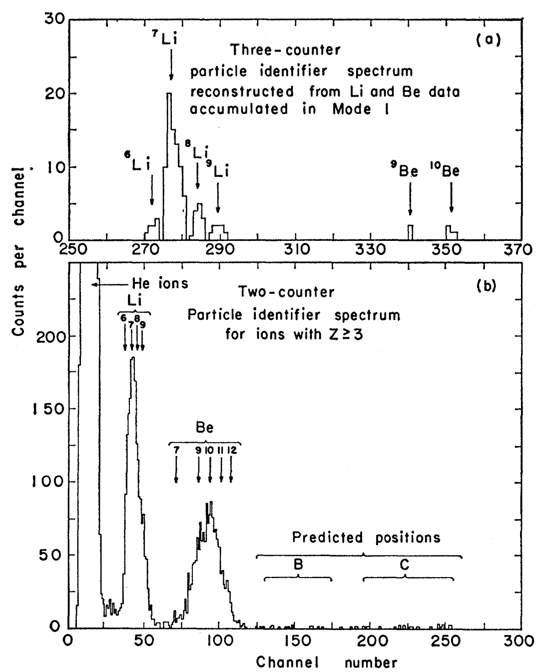

FIG. 11. (a) A three-counter particle identifier spectrum reconstructed from Li and Be ion individual events, and (b) a two-counter particle identifier spectrum showing Li and Be ion separation and predicted positions of B and C groups.

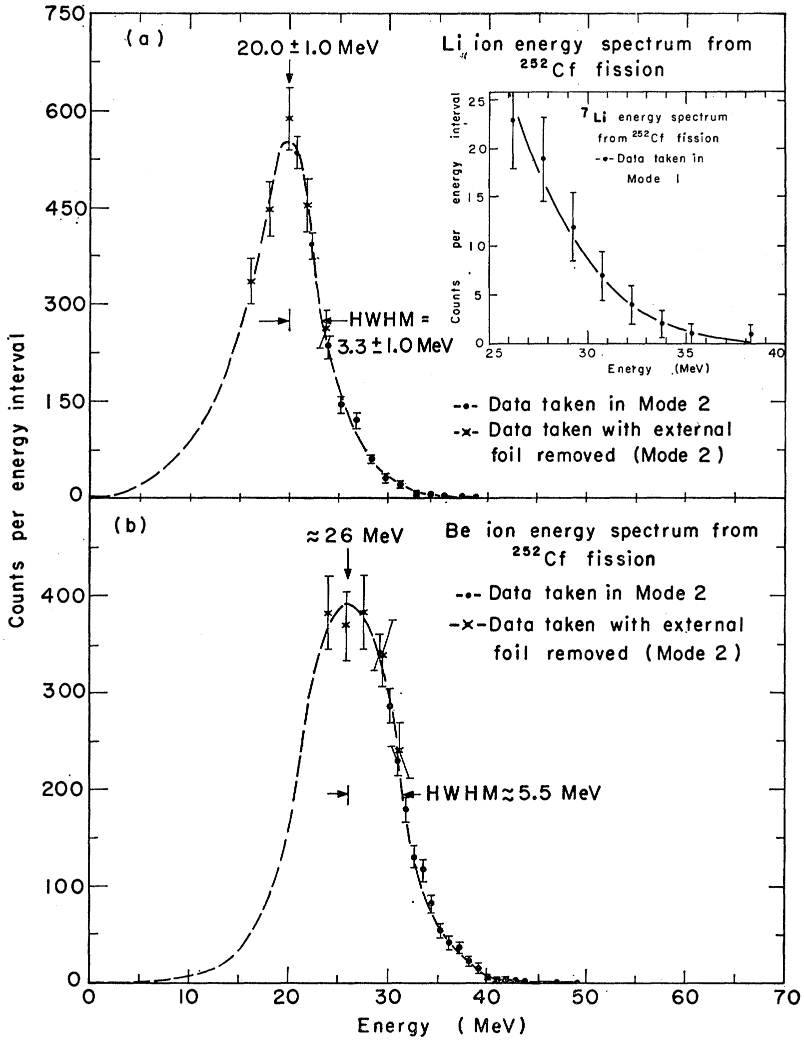

FIG. 12. Energy spectra of (a) Li and (b) Be ions emitted from ^{252}Cf fission. (a) also shows data for ^{7}Li particles taken in Mode 1. The error bars represent counting statistics only.

TABLE V. Summary of numerical data obtained from this investigation of the long-range particles emitted during the fission of ^{252}Cf.

Particle detected	Measured energy range (MeV)	Intensity relative to emission of 100 α particles[a] Measured[d]	Extrapolated[e]	Most probable energy (MeV)	HWHM (MeV)	High-energy[b] cutoff (MeV)	Uncorrected data[c] Most probable energy (MeV)	Absorber (mg/cm^2)
Proton	7.3–18.8	1.10 ±0.15	1.75 ±0.30	7.8±0.8	3.4±0.8	18.8	7.26	24.75-Au
Deuteron	5.3–21.5	0.63 ±0.03	0.68 ±0.03	8.0±0.5	3.6±0.5	22.4	7.18	24.75-Au
Triton	6.5–24.3	6.42 ±0.20	8.46 ±0.28	8.0±0.3	3.1±0.3	24.5	6.99	24.75-Au
^{3}He	14.2–21.3	≤0.075	···	···	···	···	···	8.26-Al
^{4}He	8.3–37.7	···	···	16.0±0.2	5.1±0.2	37.9	13.66	8.26-Al
^{6}He	10.0–33.3	1.95 ±0.15	2.63 ±0.18	12.0±0.5	4.0±0.5	32.6	7.85	8.26-Al
^{8}He	9.3–27.7	0.062 ±0.008	0.090±0.012	10.2±1.0	4.0±1.0	28.7	6.56	15.83-Au
^{6}Li	24.0–33.2	0.0011±0.0005	···	···	···	···	···	8.26-Al
^{7}Li	25.4–38.3	0.0081±0.0012	···	···	···	37.5	···	8.26-Al
^{8}Li	26.8–37.5	0.0015±0.0006	···	···	···	···	···	8.26-Al
^{9}Li	28.1–37.1	0.0009±0.0004	···	···	···	···	···	8.26-Al
Li ions	15.2–37.3	0.126 ±0.015	0.132±0.016	20.0±1.0	3.3±1.0	38.0	14.13	15.83-Au
^{9}Be	39.3–43.9	~0.0002	···	···	···	···	···	8.26-Al
^{10}Be	41.0–45.6	~0.0004	···	···	···	···	···	8.26-Al
Be ions	23.0–49.1	0.156 ±0.016	0.201±0.020	~26.0	~5.5	45.0	14.80	15.83-Au

[a] 299 fissions/α particle is the best available value for ^{252}Cf. See Ref. 4.
[b] These values were determined from Fig. 13.
[c] These two columns give the experimentally measured peak energies for the various distributions and the thickness and type of absorber which covered the source at the time of measurement of the peak energies.
[d] Numerical values under this column were obtained by using only those portions of the energy spectra which were determined experimentally.
[e] Numerical values under this column were obtained by using energy spectra extrapolated to zero energy as shown on the individual energy distribution graphs (see Figs. 6, 7, 10, and 12).

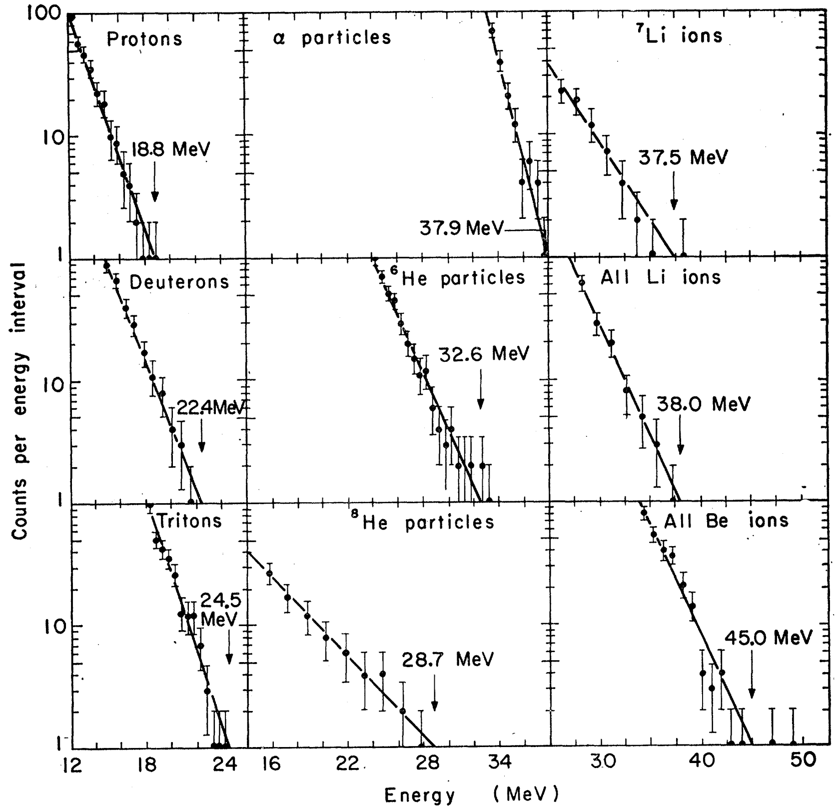

FIG. 13. End-point energy plots for particles detected from ^{252}Cf fission.

4. SUMMARY

This study of the long-range particles emitted during the fission of ^{252}Cf has confirmed[1–8] the emission of ^{1}H, ^{2}H, ^{3}H, ^{3}He, ^{4}He, and ^{6}He particles and found in addition that ^{8}He, ^{6}Li, ^{7}Li, ^{8}Li, ^{9}Li, ^{9}Be, ^{10}Be and probably some other isotopes of beryllium are also emitted. The detailed data obtained on ^{7}He, ^{9}He, and ^{10}He emission indicate that these helium isotopes are particle unstable. Energy spectra for all the observed hydrogen and helium isotopes (with the exception of ^{3}He) and for the Li and Be ions were obtained, and the most probable energy for each determined. End-point energy graphs for the various long-range particles observed in this investigation are shown in Fig. 13 where for consistency an exponential behavior of these high-energy sections has been assumed. It should be noted that the end-point energies appear to increase slowly with improving over-all statistics and hence are not necessarily reliable except as lower limits.

Relevant numerical data resulting from the "measured" and "extrapolated" energy spectra of this study are summarized in Table V, and the relative intensities of emission of the various long-range particles are shown in Fig. 14. The "measured" values resulted from using only data obtained experimentally, while the "extrapolated" values were obtained by extending each of the energy distributions to zero energy as shown by the dashed lines on the various energy spectra.

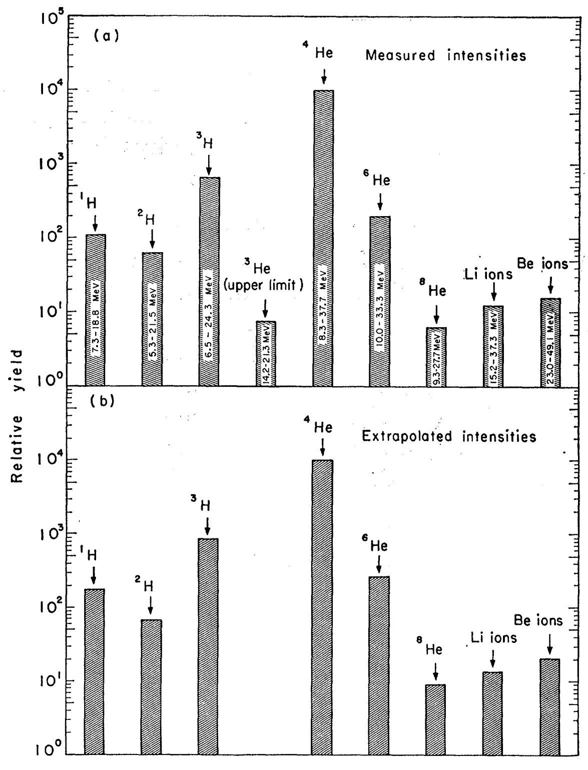

FIG. 14. Relative intensities of particles emitted from ^{252}Cf fission. The (a) measured and (b) extrapolated values are explained in the text.

ACKNOWLEDGMENTS

The authors would like to thank Dr. S. G. Thompson for his encouragement and stimulating discussion concerning this work, and also Dr. W. J. Swiatecki for several valuable discussions. We are indebted to R. M. Latimer for providing the ^{252}Cf sources, to F. S. Goulding and D. A. Landis for designing the pileup rejector and associated electronics necessary for this investigation, to C. C. Maples, Jr. for his efforts in developing the range-energy code which was vital to the experiment and to R. P. Lothrop and M. D. Roach for providing the thin transmission detectors. We would like to express our appreciation to the Lawrence Radiation Laboratory Health Chemistry Division for their efforts in the packaging and monitoring of the ^{252}Cf sources and to M. S. Coops and J. E. Evans (LRL-Livermore) for providing the ^{242}Cm source.

Note added in proof. Recently the $^7Li(t,{}^3He)^7He$ reaction has been used to show that ^7He is unbound to neutron decay ($^7He \rightarrow {}^6He + n + 420$ keV), confirming the suspected particle-instability of this nucleus [R. H. Stokes and P. G. Young (private communication)].

Errata

$^{90}Zr(p,p')$ Reaction at 18.8 MeV and the Nuclear Shell Model, W. S. GRAY, R. A. KENEFICK, J. J. KRAUSHAAR, AND G. R. SATCHLER [Phys. Rev. **142**, 735 (1966)]. Equation (4) should read

$$V_S = V_{S\alpha} + V_{S\beta}\boldsymbol{\tau}_i \cdot \boldsymbol{\tau}_p .$$

With our choice of phase for the single-particle wave functions, the ratio b/a in Eq. (9) is positive, not negative. In the multiplicative factor for the matrix elements for $p_{1/2}{}^{-1}g_{9/2}$ in Table IV the phase should be $(-)^S$, not $(-)^{J-S}$. Consequently the b terms in Eq. (10) change sign. Since the wrong sign was used for b/a, the calculations for the 5^- excitation are unaffected. Equation (11) should read

$$N_{34} = 0.396a - 0.177b ,$$
$$N_{54} = 0.044a - 0.020b ,$$

so that $N_{34} = 0.211$ and $N_{54} = 0.0234$ if $a = 0.8$, $b = 0.6$.

Shell-Model Form Factors for the $^{90}Zr(p,p')$ Reaction, M. B. JOHNSON, L. W. OWEN, AND G. R. SATCHLER [Phys. Rev. **142**, 748 (1966)]. With the coupling order $\mathbf{j} + \mathbf{j}' = \mathbf{J}$ implied by the left side of Eq. (16), the right side should be multiplied by the phase factor $(-)^{J-j-j'-1}$. The phase correction noted in the preceding erratum results in the matrix element for the $(p_{1/2}g_{9/2})$ excitation being multiplied by $[a + (-)^S(b/\sqrt{5})]$, while the cross sections for $L = 3$ shown in Fig. 5 should be multiplied by 0.44.